PNAS
www.pnas.org

Main Manuscript for

Metabolomics strategy for diagnosing urinary tract infections

Daniel B. Gregson[1,2]†, Spencer D. Wildman[3]†, Carly C.Y. Chan[3], Dominique G. Bihan[3], Ryan A. Groves[3], Thomas Rydzak[3], Keir Pittman[3], and Ian A. Lewis[3]*

[1]Department of Pathology and Laboratory Medicine, Cumming School of Medicine, University of Calgary, Calgary, AB, T2N 1N4, Canada

[2]Department of Medicine, Cumming School of Medicine, University of Calgary, Calgary, AB, T2N 1N4, Canada

[3]Department of Biological Science, University of Calgary, Calgary, AB, T2N 1N4, Canada

† Equal contributions

*Corresponding author: Ian A. Lewis

Department of Biological Sciences
2500 University Drive NW
Calgary, AB, Canada T2N 1N4
1-403-220-4366
ian.lewis2@ucalgary.ca

Author Contributions: S.D.W., C.C.Y.C., D.B.G., D.G.B., T.R., and I.A.L. designed and performed the experiments S.D.W., D.B.G., D.G.B., C.C.Y.C., R.A.G., D.B.G., and T.R. collected and interpreted mass spectrometry data. K.P. and I.A.L. interpreted results wrote the manuscript in consultation with all authors.

Competing Interest Statement: Drs. Lewis, Gregson and Mr. Groves are authors on a patent relating to the use of LC-MS for detecting urinary tract infections. No other competing interests declared.

Classification: Biological Sciences, Applied Biological Sciences

Keywords: Metabolomics; rapid diagnostic testing; infectious diseases; liquid chromatography-mass spectrometry; microbial metabolism

This file includes:

Abstract

Metabolomics has emerged as a mainstream approach for investigating complex metabolic phenotypes. Despite its obvious suitability to diagnostics, it has yet to be integrated into routine clinical laboratory applications. Metabolomics-based diagnosis of infectious diseases is a logical application of this technology since microbial metabolic waste products are concentrated at the site of infection. In the case of urinary tract infections (UTIs), one of the most common bacterial infections, microbial catabolites are trapped in the bladder and thus could enable rapid diagnosis of UTIs. We conducted an untargeted metabolomics screen of 110 clinical specimens and identified two metabolites, agmatine and N6-methyladenine, that are predictive of a wide transect of pathogen species that collectively account for over 90% of UTI infections. We showed that these metabolites were consistently observed in multiple independent cohorts, including a blinded trial of over 587 clinical specimens (95% sensitivity, 86% specificity; PPV, 0.68; NPV, 0.98). These findings demonstrate the potential utility of metabolomics for diagnosing infectious diseases. Moreover, the rapid analysis times enabled through our metabolomics diagnostic approach—six minutes per sample—could curtail the inappropriate UTI clinical prescribing practices that are currently contributing to the selection of antimicrobial resistance.

Significance statement

We show that a six-minute metabolomics assay robustly identifies most UTIs based on the presence of two microbial catabolites present in the urine. We demonstrate the potential clinical utility of this strategy in a prospective blinded trial. If implemented in clinical practice, this diagnostic approach could shorten laboratory testing times for UTIs by 18 hours and could improve antimicrobial stewardship.

Main Text

Introduction

Infections are caused by a wide range of microbes that, like all organisms, consume nutrients and secrete metabolic waste products. These microbial metabolites can be highly abundant at the site of infection (*1*) and thus could potentially serve as targets for a metabolism-based diagnostic strategy. Urinary tract infections (UTIs) are particularly amenable to this metabolic diagnostic approach because microbial metabolites are concentrated in the bladder and can be easily detected by LC-MS analysis of patient urine. *Escherichia coli*, the most common UTI pathogen, produces a variety of diamines, polyamines, and acylated conjugates of these molecules that are not typically found in human urine. These molecules have been reported as potential UTI biomarkers for over three decades (*2*, *3*), with more recent work suggesting that these amine-linked molecules may play a role in resistance to nitrosative stress in the bladder (*4*, *5*).

Although these microbial metabolites have been recognized as potential diagnostic targets for over 30 years, they have yet to be translated into a clinical diagnostic tool. The reason for this is threefold: 1) concentrations of the microbial polyamines are quite variable in urine (*6*) and are thus of borderline utility for diagnostic purposes, 2) only biomarkers of *E. coli* have been reported thus far, which is problematic because it is only one of many UTI causing organisms (*7*), and 3) LC-MS has only recently become sufficiently robust to serve as a practical diagnostic platform. The primary objective of this study was to conduct a systematic analysis of microbial metabolites found in urine from UTI patients to identify any molecules with sufficient predictive power to enable rapid, metabolic-based diagnostics. Using an untargeted LC-MS metabolomics approach, we identified two novel biomarkers that report on a wide transect of UTI pathogens and reliably predict the presence of UTIs in a blinded cohort of 587 urine samples.

Results

To identify potential biomarkers of UTIs, untargeted metabolomics analyses (Figure 1a; Table 1) of 77 infection-positive urine samples and 33 healthy control samples were conducted using

high-performance liquid chromatography-mass spectrometry (HPLC-MS). The most diagnostic features in this dataset, as judged by area under the curve (AUC) of the receiver operating characteristic (ROC) curve, were m/z 114.1025 (AUC=0.98), m/z 131.1289 (AUC=0.89), and m/z 150.0772 (AUC= 0.909; Figure 1b; Supporting dataset 1). The first two of these untargeted signals were putatively assigned to agmatine, a product of arginine metabolism (*8*), and the third was assigned to N6-methyladenine, a modified nucleobase found in prokaryotes (*9*). These assignments were validated by LC-MS/MS fragmentation patterns as well as co-elution of the target signal with analytical standards (Figure 1c).

Although both agmatine and N6-methyladenine were predictive of UTI infection, the levels of these metabolites were not uniform across UTI-causing pathogens. Infections caused by the most prominent UTI-causing *Enterobacterales* species, such as *E. coli*, were associated with elevated agmatine, whereas N6-methyladenine levels were less elevated overall, but were increased in infections caused by a small number of non-*Enterobacterales* species (Supporting dataset 1). To better understand these specifies-specific phenotypes, the performance of agmatine was assessed using 519 urine cultures that were taken directly from a clinical diagnostic pipeline, and agmatine concentrations were calculated by spiking samples with known concentrations of stable isotope labeled [U-^{13}C]agmatine prior to solid phase extraction on a silica column. Agmatine concentrations were thus quantifiable based on the signal ratio between isotope-labeled and native species. As expected, urinary agmatine levels were closely correlated with the presence of uropathogenic *Enterobacterales* (Fig. 2a; Supporting dataset 2), whereas culture-negative urine samples contained no detectable agmatine (sensitivity, 94%; specificity, 97%; PPV, 0.96; NPV, 0.95). Moreover, we found that a diagnostic threshold of 170 nM agmatine was predictive of infections caused by *E. coli*, *Citrobacter* species, *Enterobacter* species*, Klebsiella* species, and *Proteus mirabilis,* all of which showed significantly higher agmatine levels than healthy urine samples (p = 2.15×10^{-45}, p = 1.43×10^{-49}, p = 2.22×10^{-52}, p = 3.85×10^{-40}, p = 5.91×10^{-47}; Figure 2a; Supporting dataset 2).

Although the agmatine-based screening approach captures most UTI infections caused by *Enterobacterales* species—which collectively account for >83% of UTIs (*7*)—it did not capture those caused by enterococci, staphylococci, or other less common non-*Enterobacterales* pathogens. Since these pathogens account for a small percentage of all UTIs, we prospectively collected a targeted cohort of 71 non-*Enterobacterales* UTI specimens along with 24 negative controls. MS analyses showed that N6-methyladenine signals correctly differentiated culture-negative urine samples from this selected cohort of infections (sensitivity, 91%; specificity, 89%; PPV, 0.84; NPV, 0.91; Fig 2b; Supporting dataset 3). However, there were clear species-to-species differences in the quality of these metabolic diagnostics, with *Staphylococcus aureus*, *S. saprophyticus*, and *Aerococcus urinae* showing the most significant differences ($p = 1.26\times10^{-3}$, $p = 3.22\times10^{-4}$, $p = 3.72\times10^{-6}$; Figure 2b; Supporting dataset 3). N6-methyladenine is part of a wider family of adenine derivatives, including 1-methyladenine and adenine, which were elevated in the urine of these UTI patients (Supporting dataset 3). However, our MS analyses showed that the diagnostic performance of these additional markers was lower, and these compounds were linked to fewer species than N6-methyladenine.

Agmatine and N6-methyladenine in the urine of UTI patients could potentially originate from microbial or human metabolism. To better understand the origin of these molecules, filter sterilized urine was taken from healthy controls and was inoculated with *E. coli* and *S. aureus* isolates. In the case of the *E. coli* culture, 20 μM of ^{15}N-labelled arginine (a physiologically relevant level approximating the concentration of native urinary arginine) was added to the media at the start of the incubation. Throughout the incubation, isotope-labeled arginine levels progressively decreased while isotope-labeled agmatine was produced (Fig 2c). The appearance of isotope-labeled agmatine is expected under these conditions due to the microbial arginine decarboxylase activity of *E. coli* (*8*). Likewise, we screened the *S. aureus* cultures over 12 hours via LC-MS and observed that N6-methyladenine was also produced by these microbes when grown in filter-sterilized urine. In summary, the most diagnostic biomarkers observed in UTI specimens are readily produced by

UTI pathogens grown in filter-sterilized urine, indicating that these metabolites are naturally produced through microbial metabolic activity when grown in urine.

Although untargeted metabolomics is currently not used for clinical diagnostics, mass spectrometry is a routine component of many diagnostic labs where it serves as a platform for quantifying a range of biomolecules including steroid hormones, drugs of abuse, and metabolites that are linked to inborn errors of metabolism (*10*). Consequently, much of the requisite infrastructure necessary for diagnosing urinary tract infections via metabolic profiles can already be found in many diagnostic laboratories. However, both the instrumentation and methods used for untargeted metabolomics analyses are quite different from those employed in clinical settings. To demonstrate the feasibility of adapting our metabolomics approach to routine clinical diagnostics, we developed a targeted agmatine quantification workflow on a triple quadrupole LC-MS instrument that is commonly used for clinical mass spectrometry.

To determine the performance of this clinically-adapted UTI diagnostics approach, we conducted a blinded head-to-head performance evaluation of this method versus results obtained via the traditional clinical microbiology approach (*11*). This blinded cohort consisted of 587 urine specimens submitted to Alberta Precision Laboratories (South Hub) over a 48-hour period. This blinded trial confirmed our previous results: urine agmatine levels over the threshold of 170 nM correctly predicted most *Enterobacterales* infections (95% sensitivity, 86% specificity; PPV, 0.68; NPV, 0.98; Fig. 3, Supporting dataset 4). As expected, our culture-negative samples, those classified as doubtful clinical significance, and a small number of urine samples (<5%) containing non-*Enterobacterales* microbes all had agmatine levels below the limit of detection. In summary, our clinically-adapted diagnostic strategy correctly identified *Enterobacterales* infections in a large-scale blinded cohort of samples.

Discussion

Metabolomics has emerged as a mainstream research approach for understanding complex biological phenomena. Although metabolomics has been widely recognized as a potentially powerful tool for clinical diagnostics, it has yet to be integrated in routine clinical diagnostics. Here

we show a practical approach for diagnosing urinary tract infections by quantifying the concentrations of microbially-derived catabolites present in the urine. We show that two compounds, agmatine and N6-methyladenine, are sufficient for diagnosing infections caused by more than 14 species of microbes (Supporting datasets 2–3), which are collectively responsible for over 90% of UTI infections (*7*).

Although there are a range of well-established tools available for diagnosing urinary tract infections, the mass spectrometry-based approach introduced here offers some significant advantages for clinical diagnostic applications. The current approach for detecting UTIs in clinical laboratories is a multi-day, resource-intensive procedure which requires an eighteen-hour bacterial culture step before a preliminary UTI diagnosis can be made (*11*). These significant delays mean that antibiotics are prescribed before lab results are available, a practice which is thought to contribute to the selection and spread of antimicrobial resistant microbes (*12*–*14*). Our metabolomics approach is advantageous in that it detects microbial metabolites in the original urine specimen, and thus would require less sample handling and much less time than is needed for the existing pipeline. The targeted metabolomics-based screening methods used here cut the positive/negative screening timeline down to as little as six minutes per sample—over 18 hours faster than the established culture-based pipeline—and can be performed on existing medical device compliant LC-MS systems. This major performance improvement could have significant implications for proper antibiotic stewardship in the treatment of UTIs.

In summary, we conducted a comprehensive analysis of metabolites found in clinical urine specimens and found that two metabolites present in the urine, agmatine and N6-methyladenine, are predictive of UTIs. We showed that these molecules result from natural microbial metabolic processes when these organisms are grown in urine. In addition, we developed a clinically-adapted analytical workflow that follows the established conventions used in clinical mass spectrometry. Using this refined method, we showed that our metabolic diagnostic strategy performs well when applied to large-scale clinical cohorts and could be realistically implemented in large-scale clinical laboratories. The significant time savings enabled by this approach could have important impacts

on both the practical operations of diagnostic laboratories as well as improving antibiotic stewardship practices in the management of UTIs.

Materials and Methods

Urine sample collection

Mid-stream urine samples were collected from Alberta Precision Laboratories' (APL) standardized urine analysis workflow. In brief, urine was plated either manually with a loop or using automated equipment onto UriSelect™ Media (Bio-Rad, Canada) and incubated aerobically for 18 hours. Growth of bacteria was enumerated as per standard recommendations (*11*) and colonies present in significant quantities were speciated using the Vitek™ MS system (bioMérieux, Canada). Residual samples from this standard diagnostic lab workflow were fixed in 50% methanol within 48 hours post-receipt at APL, and then frozen at -80 °C. All samples were acquired under approval from Conjoint Health Research Ethics Board certificate REB16-0167. Prior to untargeted analysis, samples were thawed, centrifuged at 14,800 × g, and diluted ten-fold further into 50% HPLC-grade methanol.

Untargeted mass spectrometry

The methods used here have been adapted from previously published studies (*15*, *16*). Briefly, metabolic analyses were performed on a Q Exactive™ HF Hybrid Quadrupole-Orbitrap™ Mass Spectrometer (Thermo-Fisher) coupled to a Vanquish™ UHPLC System (Thermo-Fisher). Chromatographic separation of metabolites was performed on Syncronis HILIC UHPLC column (2.1mm x 100mm x 1.7µm, Thermo-Fisher) at a flow rate of 600µL/min using a binary solvent system: solvent A, 20mM ammonium formate pH 3.0 in mass spectrometry grade H_2O and solvent B, mass spectrometry grade acetonitrile with 0.1% formic acid (%v/v). For initial biomarker discovery experiments, the following 15-minute gradient was used: 0–2 min, 100% B; 2–7 min, 100–80% B; 7–10 min, 80–5% B; 10–12 min, 5% B; 12–13 min, 5–100% B; 13–15 min, 100% B. The mass spectrometer was run in positive and negative full scan mode at a resolution of 240,000 scanning from 50-750m/z. Metabolite data were analyzed by El-MAVEN software package (*17*, *18*). Metabolites were identified by matching observed m/z signals (+/-10ppm) and

chromatographic retention times to those observed from commercial metabolite library of standards (MSMLS; Sigma-Aldrich). Assignments were verified on the Thermo Fisher Q Exactive™ HF platform via MS/MS fragmentation analysis and co-elution of standards with the identified signals from urine.

Targeted mass spectrometry

Quantitative analyses of agmatine in urine samples was undertaken using a known concentration of a [U-13C]agmatine isotope as an internal standard in the urine sample (see [U-13C]agmatine standard biosynthesis and purification below). Prior to MS analysis, samples were purified using a 96-well HyperSep™ Silica plate. Columns were equilibrated with methanol followed by water, then loaded with the sample of interest. Columns were then washed with methanol, water, methanol with 0.1% formic acid, water with 0.1% formic acid. The target analyte was eluted with water containing 2% formic acid. LC-MS analysis was performed using a TSQ Quantum™ Access MAX Triple Quadrupole Mass Spectrometer (Thermo Scientific). For the clinically-adapted blinded evaluation, clinical urine specimens were centrifuged and the supernatant was spiked with the [U-^{13}C]agmatine isotope. These samples were analyzed directly on a TSQ Quantum™ Access MAX instrument.

For all quantitative analyses, the following transitions were monitored using a fixed collision energy of 15eV: ^{12}C agmatine, 131.2->72.4m/z; [U-^{13}C]agmatine, 136.2->76.4m/z in positive ionization mode. The same HPLC column and buffers were used as described above, with the following modified 6-minute gradient: 0–0.5 min, 100% B; 0.5–2 min, 100–5% B; 2–3.5 min, 5–0% B; 3.5–4.5 min, 0% B; 4.5–5 min, 0–100% B; 5–6 min, 100% B. Electrospray ionization source conditions were as follows: spray voltage of 3000 V, sheath gas of 25 (arbitrary units), auxiliary gas of 10 (arbitrary units), sweep gas of 0 (arbitrary units), capillary temperature of 275°C, auxiliary gas temperature of 325 °C.

[U-^{13}C]agmatine standard biosynthesis and purification

Escherichia coli (strain MG1665) was seeded into M9 minimal media containing 22.2 mM [U-^{13}C]glucose, grown overnight, and was then seeded into fresh [U-^{13}C]glucose-containing media.

This culture was then incubated under agitation in a 37 °C, 5% CO_2 incubator. Glucose consumption was monitored using a blood glucose monitoring system (Bayer Contour Next). When glucose levels in the media reached 5 mM, the culture was centrifuged, the supernatant was retrieved, was adjusted to pH 7 with ammonium bicarbonate, and was steri-filtered. [U-^{13}C]agmatine was isolated and purified using a solid phase extraction column (HyperSep™ Silica Cartridges, # 60108-712, Thermo Scientific), as described above and scaled accordingly to the column volume. The fraction was concentrated to 1/10th of its initial volume in a vacuum concentrator at 4 °C and labeled [U-^{13}C]agmatine in the final sample was quantified by stable isotope dilution via LC-MS/MS using an unlabeled internal standard curve.

E. coli and Staphylococcus aureus urine cultures

In vitro microbial samples were cultured from reference strains of bacteria (*E. coli*: MG1665, ATCC 25922, ESBL ATCC BAA-196; *S. aureus*: ATCC25923, ATCC 43300 (MRSA)). Briefly, cryogenic stocks were grown overnight in Mueller-Hinton medium, then inoculated at 10^5 CFU/mL in sterilized urine and grown at 37 °C. *E. coli* cultures were spiked with [guanido$^{15}N_2$]arginine (herein referred to as "[$^{15}N_2$]arginine") such that the urine contained an approximate 1:1 ^{12}C arginine to [$^{15}N_2$]arginine ratio. The disappearance of [$^{15}N_2$]-arginine and appearance of [guanido-$^{15}N_2$]agmatine (herein referred to as "[$^{15}N_2$]agmatine") was monitired over four hours using LC-MS/MS. Similarly, the appearance of N6-methyladenine signal was assessed in *S. aureus* cultures at 0, 4, 8, 10, and 12 hours.

Blinded performance evaluation of agmatine versus traditional urine analysis pipeline

Mid-stream urine samples for the blinded head-to-head performance evaluation were collected from Alberta Precision Laboratories' standardized urine analysis workflow (described above in *Urine Sample Collection*). These samples were stripped of diagnostic information and assigned a unique identifier prior to their transfer to the analytical team. Following analysis using clinically adapted metabolomics platform, diagnostic data were un-masked and the results of the quantitative agmatine-based MS approach were scored against the clinical diagnostic laboratory calls, using 170nM as the threshold for UTI-positive samples.

Data analysis and statistics

Raw mass spectrometry files were converted into .mzXML files via MSConvertGUI (ProteoWizard Tools) (*19*). All full scan MS analyses were conducted in MAVEN. MS/MS data were analyzed using Xcalibur 4.0.27.19 software (Thermo Scientific). Untargeted mass spectrometry data were grouped according to co-variance, co-retention and similarity to common adducts/fragments using previously published software developed in R Statistics (*20*). Violin plots, ROC curves, and scatter plots were all generated in R Statistics using existing packages, (pROC and vioPlot). All data is available upon request from the study team.

Acknowledgments

This work was supported by Genome Canada (10019200), the Canadian Institute of Health Research (162790), the University of Calgary (Biomedical Engineering 10011121), and Alberta Precision Laboratories. I.A.L is supported by an Alberta Innovates Translational Health Chair. T.R. is supported by an Eyes-High Postdoctoral Fellowship from the University of Calgary. S.D.W. was supported in part by an NSERC Undergraduate Summer Research Award. Metabolomics data were acquired at the Calgary Metabolomics Research Facility, which is supported by the International Microbiome Centre and the Canada Foundation for Innovation (CFI-JELF 34986).

References

1. M. Fernández-García, D. Rojo, F. Rey-Stolle, A. García, C. Barbas, in *Metabolic Interaction in Infection*, R. Silvestre, E. Torrado, Eds. (Springer International Publishing, Cham, 2018; https://doi.org/10.1007/978-3-319-74932-7_7), pp. 283–315.
2. H. P. W. M. Satink, J. Hessels, A. W. Kingma, G. A. van den Berg, F. A. J. Muskiet, M. R. Halie, Microbial influences on urinary polyamine excretion. *Clin. Chim. Acta*. 179, 305–314 (1989).
3. M. Lussu, T. Camboni, C. Piras, C. Serra, F. Del Carratore, J. Griffin, L. Atzori, A. Manzin, 1H NMR spectroscopy-based metabolomics analysis for the diagnosis of symptomatic E. coli-associated urinary tract infection (UTI). *BMC Microbiol.* 17, 201 (2017).
4. J. M. Bower, M. A. Mulvey, Polyamine-Mediated Resistance of Uropathogenic Escherichia coli to Nitrosative Stress. *J. Bacteriol.* 188, 928–933 (2006).
5. S. Puebla-Barragan, J. Renaud, M. Sumarah, G. Reid, Malodorous biogenic amines in Escherichia coli-caused urinary tract infections in women—a metabolomics approach. *Sci. Rep.* 10, 9703 (2020).
6. S. Bouatra, F. Aziat, R. Mandal, A. C. Guo, M. R. Wilson, C. Knox, T. C. Bjorndahl, R. Krishnamurthy, F. Saleem, P. Liu, Z. T. Dame, J. Poelzer, J. Huynh, F. S. Yallou, N. Psychogios, E. Dong, R. Bogumil, C. Roehring, D. S. Wishart, The Human Urine Metabolome. *PLoS One*. 8 (2013), doi:10.1371/journal.pone.0073076.
7. K. B. Laupland, T. Ross, J. D. D. Pitout, D. L. Church, D. B. Gregson, Community-onset Urinary Tract Infections: A Population-based Assessment. *Infection*. 35, 150 (2007).
8. C.-D. Lu, Pathways and regulation of bacterial arginine metabolism and perspectives for obtaining arginine overproducing strains. *Appl. Microbiol. Biotechnol.* 70, 261–272 (2006).
9. S. S. Mohapatra, E. G. Biondi, in *Cellular Ecophysiology of Microbe*, T. Krell, Ed. (Springer International Publishing, Cham, 2017; https://doi.org/10.1007/978-3-319-20796-4_23-1), pp. 1–21.

10. J. E. Adaway, B. G. Keevil, L. J. Owen, Liquid chromatography tandem mass spectrometry in the clinical laboratory. *Ann. Clin. Biochem.* 52, 18–38 (2014).

11. W. W. Chan, in *Clinical Microbiology Procedures Handbook*, A. L. Leber, Ed. (ASM Press, Washington, DC, ed. 4th, 2016), p. p 3.12.1-3.12.33.

12. A. H. Holmes, L. S. P. Moore, A. Sundsfjord, M. Steinbakk, S. Regmi, A. Karkey, P. J. Guerin, L. J. V Piddock, Understanding the mechanisms and drivers of antimicrobial resistance. *Lancet*. 387, 176–187 (2016).

13. D. I. Andersson, D. Hughes, Microbiological effects of sublethal levels of antibiotics. *Nat. Rev. Microbiol.* 12, 465 (2014).

14. C. Costelloe, C. Metcalfe, A. Lovering, D. Mant, A. D. Hay, Effect of antibiotic prescribing in primary care on antimicrobial resistance in individual patients: systematic review and meta-analysis. *BMJ*. 340, c2096 (2010).

15. L. F. Mager, R. Burkhard, N. Pett, N. C. A. Cooke, K. Brown, H. Ramay, S. Paik, J. Stagg, R. A. Groves, M. Gallo, I. A. Lewis, M. B. Geuking, K. D. McCoy, Microbiome-derived inosine modulates response to checkpoint inhibitor immunotherapy. *Science (80-.).* 369, 1481–1489 (2020).

16. X. Dong, J. E. Rattray, D. C. Campbell, J. Webb, A. Chakraborty, O. Adebayo, S. Matthews, C. Li, M. Fowler, N. M. Morrison, A. MacDonald, R. A. Groves, I. A. Lewis, S. H. Wang, D. Mayumi, C. Greening, C. R. J. Hubert, Thermogenic hydrocarbon biodegradation by diverse depth-stratified microbial populations at a Scotian Basin cold seep. *Nat. Commun.* 11, 5825 (2020).

17. M. F. Clasquin, E. Melamud, J. D. Rabinowitz, *Curr. Protoc. Bioinforma.*, in press, doi:10.1002/0471250953.bi1411s37.

18. E. Melamud, L. Vastag, J. D. Rabinowitz, Metabolomic Analysis and Visualization Engine for LC−MS Data. *Anal. Chem.* 82, 9818–9826 (2010).

19. M. C. Chambers, B. Maclean, R. Burke, D. Amodei, D. L. Ruderman, S. Neumann, L. Gatto, B. Fischer, B. Pratt, J. Egertson, K. Hoff, D. Kessner, N. Tasman, N. Shulman, B.

Frewen, T. A. Baker, M.-Y. Brusniak, C. Paulse, D. Creasy, L. Flashner, K. Kani, C. Moulding, S. L. Seymour, L. M. Nuwaysir, B. Lefebvre, F. Kuhlmann, J. Roark, P. Rainer, S. Detlev, T. Hemenway, A. Huhmer, J. Langridge, B. Connolly, T. Chadick, K. Holly, J. Eckels, E. W. Deutsch, R. L. Moritz, J. E. Katz, D. B. Agus, M. MacCoss, D. L. Tabb, P. Mallick, A cross-platform toolkit for mass spectrometry and proteomics. *Nat. Biotechnol.* 30, 918 (2012).

20. R Core Team, R: A Language and Environment for Statistical Computing (2019), (available at https://www.r-project.org).

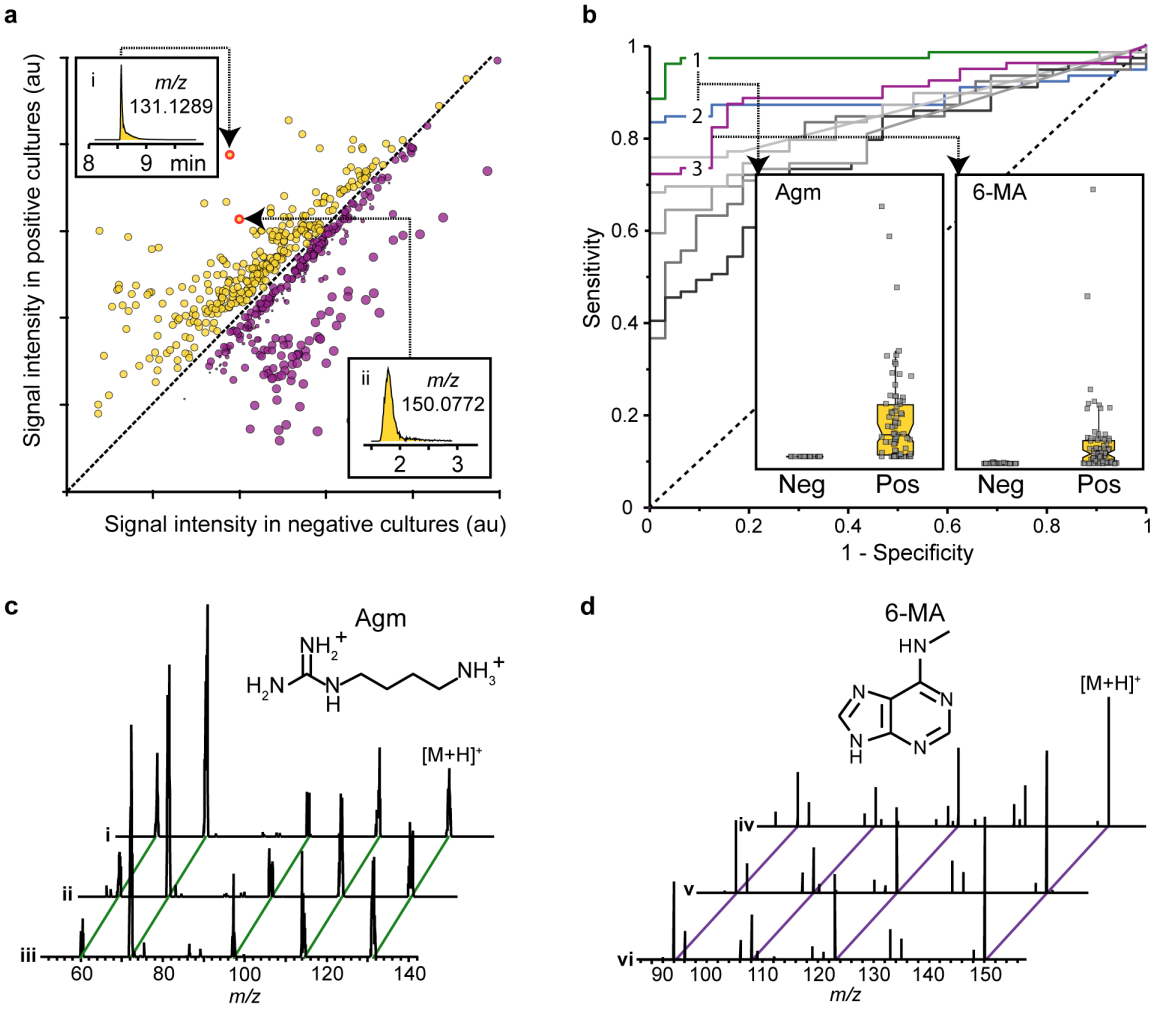

Fig. 1. Discovery of agmatine and N6-methyladenine as UTI biomarkers. (a) LC-MS data were acquired from metabolites predictive of culture-positive (yellow points) and culture-negative (purple points) urine samples. Potential UTI biomarkers were identified (*m/z* 131.1289 and *m/z* 150.0772 shown as example; see inset for chromatogram). (**b)** Predictive UTI biomarkers were ranked according to receiver operator characteristic (ROC) curves. Signal 1 (*m/z* 114.1025) and signal 2 (*m/z* 131.1289) were assigned to agmatine, and signal 3 (*m/z* 150.0771) was assigned to N6-methyladenine. **(c)** Agmatine and **(d)** N6-methyladenine assignments were verified by tandem LC-MS/MS fragmentation patterns observed in a culture-positive urine sample (i, iv), an analytical standard of the target molecule (ii; 250 nM, v; 50 μM), and a standard added to a culture-negative urine sample at the same concentration (iii, vi).

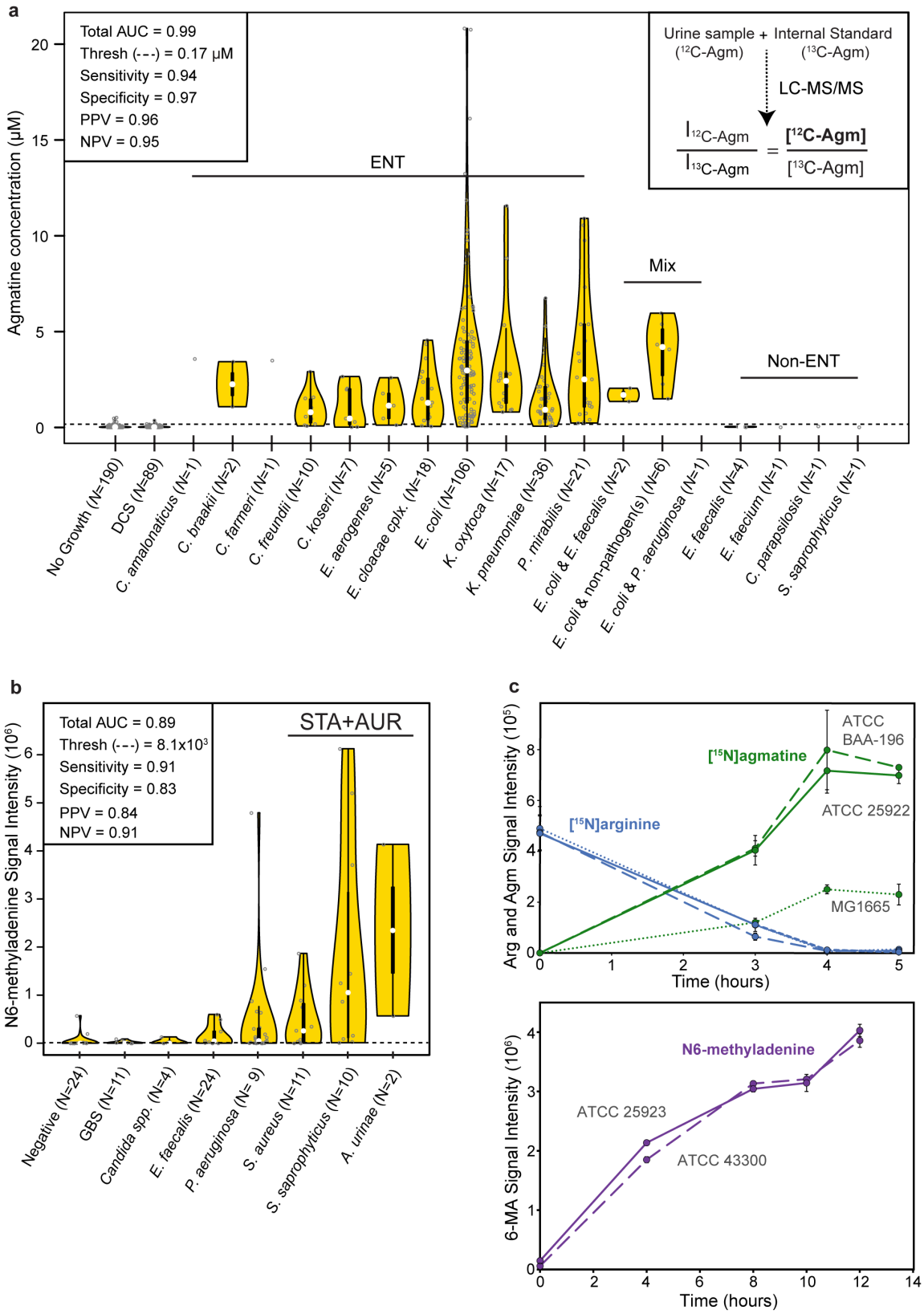

Fig. 2 Microbial metabolite signals differentiate *Enterobacterales* and non-*Enterobacterales* positive urines from controls. (a) Violin plot of agmatine concentrations in urine samples determined by spike-in of stable isotope-labeled internal standard (see inset). White dots indicate median values, thick black bars indicate interquartile ranges, and thin black lines indicate 3x interquartile hinge points. **(b)** Violin plot of N6-methyladenine signal intensities from a prospectively collected non-*Enterobacterales* cohort of patient urine samples. **(c)** Three *E. coli* strains grown in sterile urine spiked with [$^{15}N_2$]arginine for eight hours (top) were monitored for [$^{15}N_2$]agmatine production. Two *S. aureus* strains grown in sterile urine for 12 hours (bottom) and were monitored for N6-methyladenine production. Abbreviations: Agm, agmatine, AUC, area under curve; Thresh, threshold; PPV, positive predictive value, NPV, negative predictive value; DCS, doubtful clinical significance; Non-ENT, Non-*Enterobacterales*; ENT, *Enterobacterales*; Mix, polymicrobial cultures containing at least one *Enterobacterales* member; STA, *Staphylococcus* species; AUR, *A. urinae*.

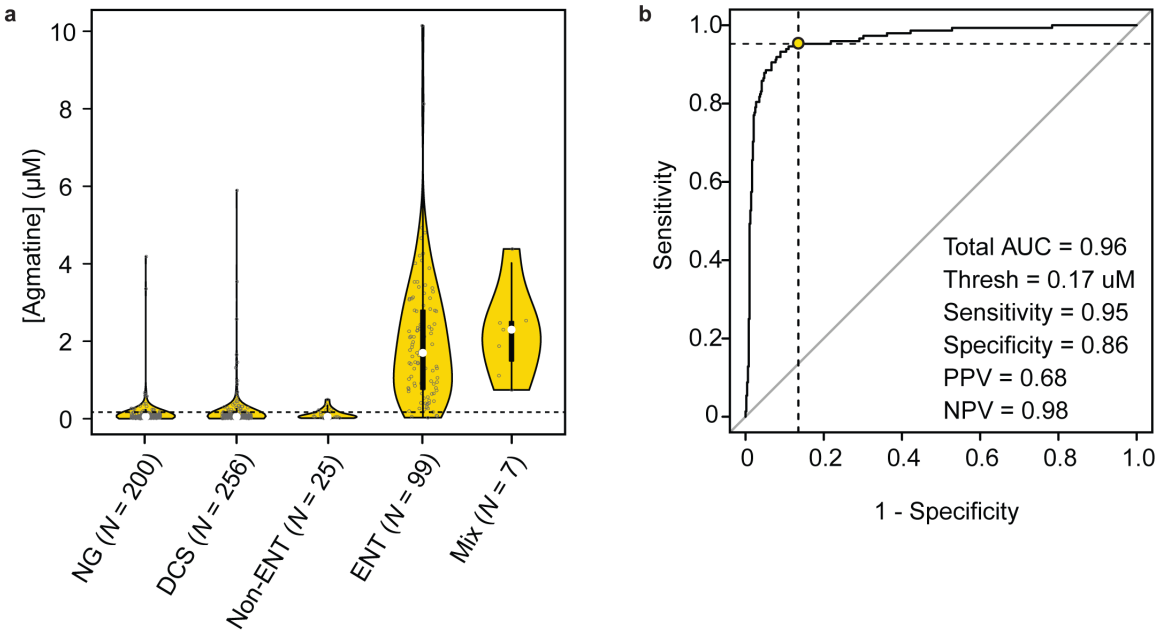

Figure 3. Blinded performance trial of clinically adapted, metabolomics-based UTI diagnostics. (a) Agmatine concentrations in a blinded cohort of clinical urine samples. Categories on x-axis represent calls from traditional microbiology analysis performed at a regional diagnostic lab. (**b)** Receiver operator curve demonstrating the performance of agmatine as a diagnostic marker for *Enterobacterales* in a blinded, prospective trial. Sensitivity and specificity for 0.17 μM threshold is represented by the yellow dot. Abbreviations: NG, no growth; DCS, doubtful clinical significance; Non-ENT, Non-*Enterobacterales*; ENT, *Enterobacterales*; Mix, polymicrobial cultures containing at least one *Enterobacterales* member; AUC, area under curve; Thresh, threshold; PPV, positive predictive value, NPV, negative predictive value.

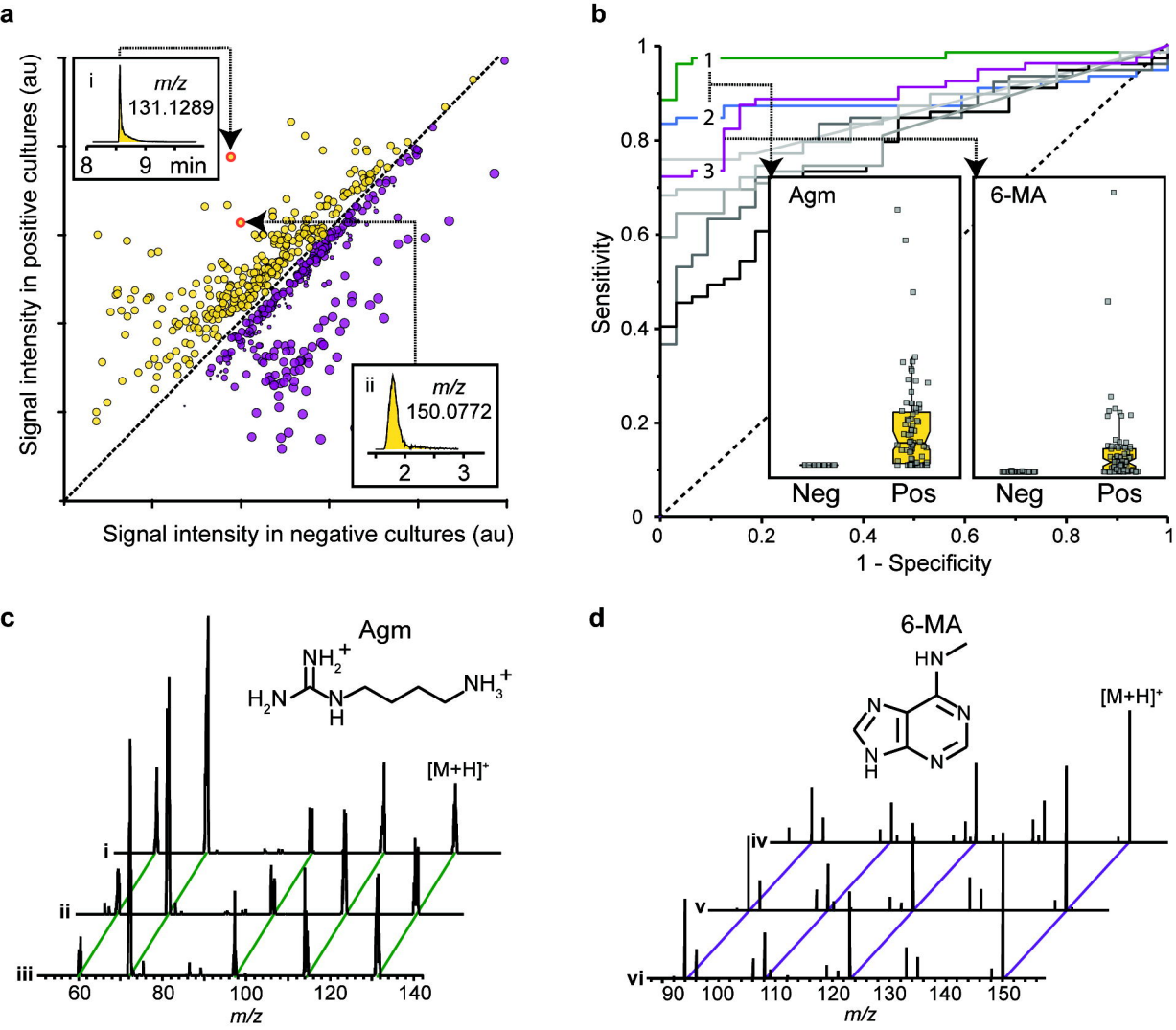
a
Signal intensity in positive cultures (au)
Signal intensity in negative cultures (au)
i
m/z
131.1289
8
9
min
ii
m/z
150.0772
2
3
b
Sensitivity
1 - Specificity
1
2
3
Agm
6-MA
Neg
Pos
Neg
Pos
c
Agm
[M+H]+
i
ii
iii
60
80
100
120
140
m/z
d
6-MA
[M+H]+
iv
v
vi
90
100
110
120
130
140
150
m/z

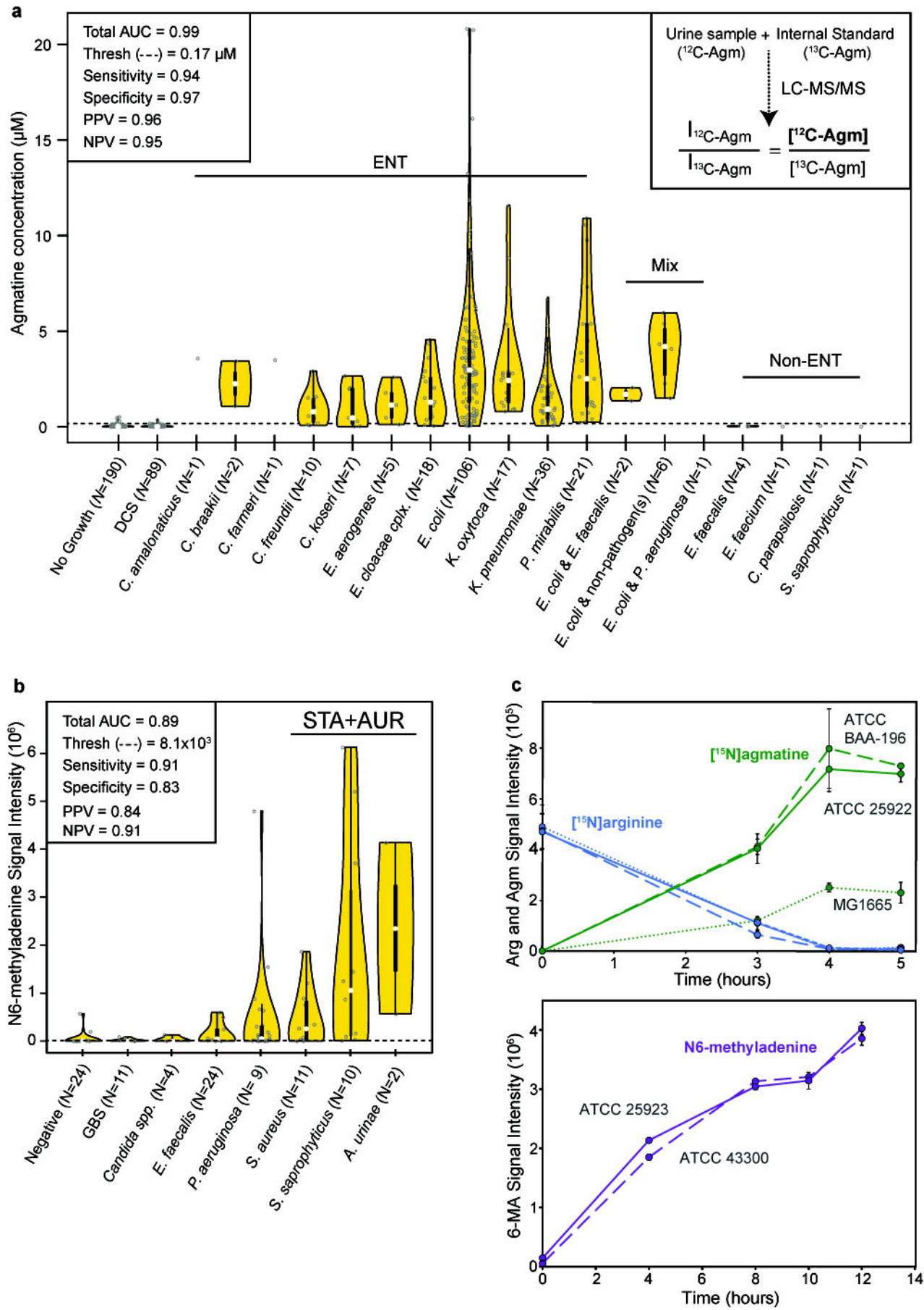
a
Total AUC = 0.99
Thresh (---) = 0.17 µM
Sensitivity = 0.94
Specificity = 0.97
PPV = 0.96
NPV = 0.95
Urine sample + Internal Standard
(12C-Agm) (13C-Agm)
LC-MS/MS
I12C-Agm / I13C-Agm = [12C-Agm] / [13C-Agm]
Agmatine concentration (µM)
ENT
Mix
Non-ENT
No Growth (N=190)
DCS (N=89)
C. amalonaticus (N=1)
C. braakii (N=2)
C. farmeri (N=1)
C. freundii (N=10)
C. koseri (N=7)
E. aerogenes (N=5)
E. cloacae cplx. (N=18)
E. coli (N=106)
K. oxytoca (N=17)
K. pneumoniae (N=36)
P. mirabilis (N=21)
E. coli & E. faecalis (N=2)
E. coli & non-pathogen(s) (N=6)
E. coli & P. aeruginosa (N=1)
E. faecalis (N=4)
E. faecium (N=1)
C. parapsilosis (N=1)
S. saprophyticus (N=1)
b
Total AUC = 0.89
Thresh (---) = 8.1x10³
Sensitivity = 0.91
Specificity = 0.83
PPV = 0.84
NPV = 0.91
STA+AUR
N6-methyladenine Signal Intensity (10⁶)
Negative (N=24)
GBS (N=11)
Candida spp. (N=4)
E. faecalis (N=24)
P. aeruginosa (N= 9)
S. aureus (N=11)
S. saprophyticus (N=10)
A. urinae (N=2)
c
Arg and Agm Signal Intensity (10⁵)
[15N]agmatine
[15N]arginine
ATCC BAA-196
ATCC 25922
MG1665
Time (hours)
6-MA Signal Intensity (10⁶)
N6-methyladenine
ATCC 25923
ATCC 43300
Time (hours)

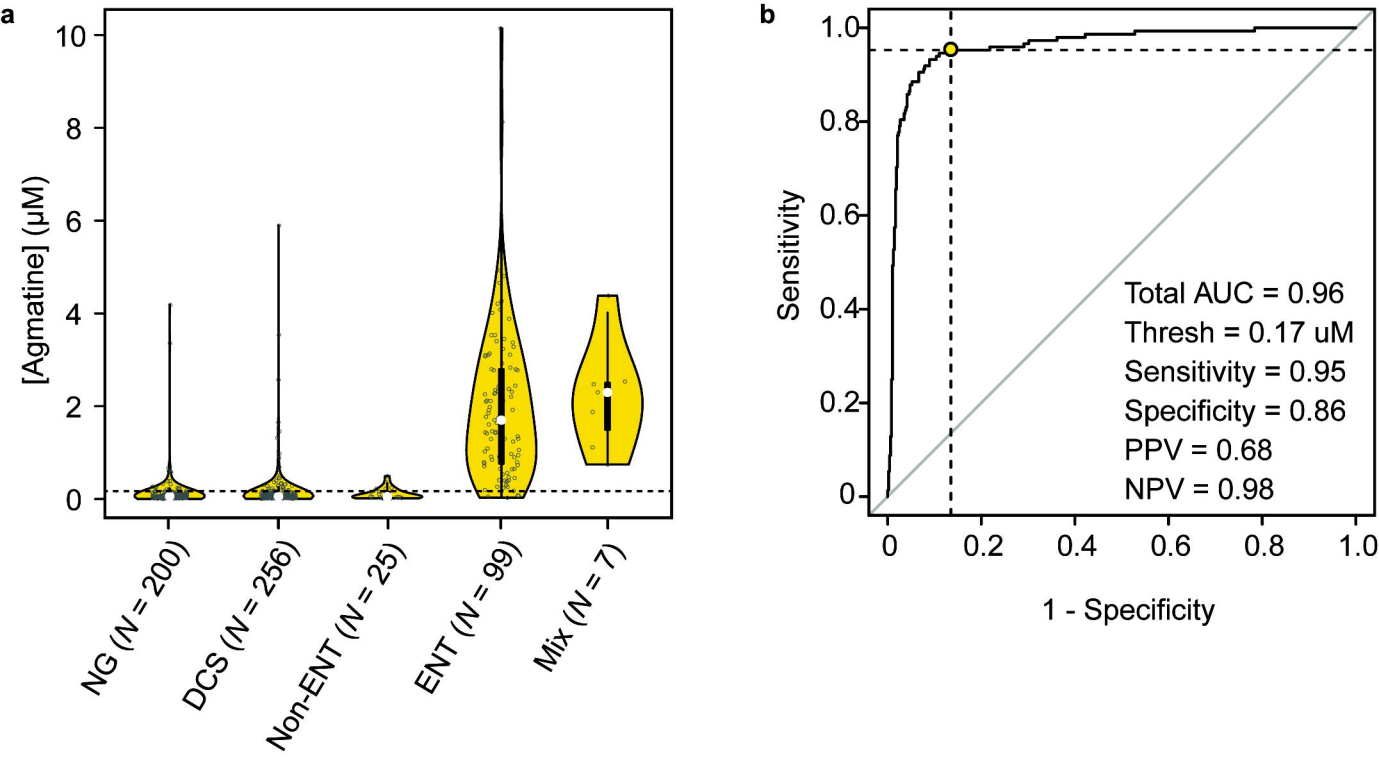
a
[Agmatine] (μM)
0
2
4
6
8
10
NG (N = 200)
DCS (N = 256)
Non-ENT (N = 25)
ENT (N = 99)
Mix (N = 7)
b
Sensitivity
0
0.2
0.4
0.6
0.8
1.0
1 - Specificity
Total AUC = 0.96
Thresh = 0.17 uM
Sensitivity = 0.95
Specificity = 0.86
PPV = 0.68
NPV = 0.98